scientific reports

Check for updates

OPEN

Combined *f*MRI and eye-tracking evidence on the neural processing of visual ambiguity in photographic aesthetics

Maria Arioli[1], Nicola Canessa[2,3]✉, Alessandra Gargiulo[4], Matteo Zardin[5], Andrea Falini[6,7] & Alberto Sanna[5]

While visual ambiguity is known to play a central role in modern art, the neural correlates of its processing remain substantially unexplored in the case of aesthetic stimuli. To fill this gap, we combined eye-tracking and functional magnetic resonance imaging (*f*MRI) to investigate both visual exploration, and the associated brain activity and connectivity, when observing (WO) or evaluating (WE) either ambiguous (AMB+) or non-ambiguous (AMB-) artistic photographic stimuli. These manipulations highlighted more fixations (suggestive of higher loading on exploratory processes) when evaluating compared with observing, and stronger right fronto-parietal and occipito-temporal activity (possibly supporting the resolution of visual ambiguity through attentional reorienting to global vs. local aspects) when processing ambiguous compared with non-ambiguous stimuli. Task-by-stimulus type interaction analyses showed that evaluating ambiguous stimuli was specifically associated with stronger fixation-related activity in the left medial prefrontal cortex, as well as decreased connectivity from this region to its right-hemispheric homologue, possibly supporting in-depth visuospatial analyses of complex visual images. These findings pave the way for future studies addressing the role of visual ambiguity in aesthetic appreciation, as well as the factors that might ease vs. hamper its processing and resolution, and their neural correlates.

Keywords Neuroaesthetics, Visual ambiguity, *f*MRI, Eye-tracking, Superior parietal lobule, Medial prefrontal cortex

Neuroaesthetics is a growing field aimed to highlight the neural correlates of aesthetic experience and appreciation[1]. This goal is typically pursued with participants reporting aesthetic judgments of visual artworks (i.e., visual aesthetic experience (VAE);[2]) while the associated brain activity is recorded via neuroimaging techniques such as functional magnetic resonance imaging (*f*MRI; e.g.,[3]). The available evidence shows that VAE entails a flexible interaction among three main brain systems (i.e., *aesthetic triad*;[4]), usually referred to as the sensory-motor, the emotion-valuation and the meaning-knowledge systems[5,6]. In particular, different categories of visual art appear to involve specific components of the sensory-motor system, such as the fusiform face area for portraits, the parahippocampal place area for landscapes, as well as the supplementary motor area and the insula for body sculptures[7]. This activation pattern is considered to support the engagement of embodied mechanisms in art comprehension and appreciation[8,9]. The key-nodes of the emotion-valuation system, including ventral striatum, insula, orbitofrontal cortex and anterior cingulate cortex, are considered to underpin the pleasure inherent in, and thus the search for, a subjectively rewarding VAE[10]. The latter is also shaped, however, by exogenous and endogenous factors such as contextual information under which artworks are presented (e.g., gallery vs. computer;[11]), culture (e.g., Eastern vs. Western;[12]), and individual art expertise

[1]Department of Human and Social Sciences, University of Bergamo, Bergamo 24129, Italy. [2]IUSS Cognitive Neuroscience (ICoN) Center, Scuola Universitaria Superiore IUSS, Pavia 27100, Italy. [3]Cognitive Neuroscience Laboratory of Pavia Institute, Istituti Clinici Scientifici Maugeri IRCCS, Pavia 27100, Italy. [4]Fondazione Centro San Raffaele, Via Olgettina, 60, Milan 20132, Italy. [5]Center for Advanced Technology in Health and Well-Being, IRCCS Ospedale San Raffaele, Via Olgettina, 60, Milan 20132, Italy. [6]Vita-Salute San Raffaele University, Milan, Italy. [7]Neuroradiology Unit and CERMAC, IRCCS Ospedale San Raffaele, Milan, Italy. ✉email: nicola.canessa@iusspavia.it

(e.g., expert vs. novices;[13,14]), which highlights the engagement of key nodes of the meaning-knowledge system such as the precuneus and the frontopolar cortex[15].

The responsiveness of these brain systems is modulated by multiple *aesthetic factors* (i.e., variables known for their effect on aesthetic preferences;[16–18]), as shown by their stronger activation for stimuli characterized by symmetric and smoothly-curved shapes, that are typically preferred over those characterized by asymmetric[19] and angular[20,21] contours.

Another likely driver of the aesthetic experience is *visual ambiguity*, i.e., the stimulus quality of being open to more than one interpretation[22,23]. Importantly, however, mixed results have been published regarding this effect on aesthetic preferences. On the one hand, some studies have reported a stronger appreciation for non-ambiguous and familiar stimuli that are fluently processed (i.e., *fluency account for aesthetics*;[24]), while others reported an opposite effect, i.e., that ambiguous stimuli might be liked more, and considered more interesting, than non-ambiguous ones[25–28]. Regardless of the direction of this preference—which is probably subject to individual differences[29,30]—it is surprising that the neural correlates of the effect of visual ambiguity on aesthetic appreciation have been only marginally investigated. To the best of our knowledge, indeed, this topic has been addressed only by two studies, reporting that the aesthetic evaluation of ambiguous paintings, such as Arcimboldo's portraits, selectively involved the right superior parietal cortex, likely supporting the integration of aesthetic experience and perceptual processing of the attended stimuli[31,32]. These studies provided a robust ground for the inquiry on other possible facets of the effect of visual ambiguity on VAE. One such facet is represented by the reward inherent in the challenging attempt to resolve visual ambiguity in artistic stimuli[27,33], as in the case of Baranowski's street art or Suissas' photos (for an overview of ambiguity in modern art, see[34–36].

Investigating the mechanisms underlying the resolution of art ambiguity might also provide novel insights into the neural dynamics of flexibility and adaptation. While ambiguity resolution is mastered by most individuals as a mean to act effectively in our everyday environment[37], and to enable new forms of efficient behaviour[23], still it is pursued with strategies that largely differ across individuals both in normal and pathological conditions[38]. In the latter case, an impairment of this ability in conditions such as Parkinson's disease[39], dyslexia[40] and schizophrenia[41] severely worsens patients' quality of life.

It is thus crucial to unveil the brain areas associated with the processing and the resolution of visual ambiguity, that have been so far investigated mostly with non-artistic stimuli[37]. The available data highlighted a distributed brain network involving sectors of the occipito-temporal cortex—including the fusiform gyrus and the lateral occipital cortex[42]—alongside the prefrontal cortex[43,44] and fronto-parietal areas[45,46]. Interestingly, their engagement is also shaped by specific stimuli features, such as ambiguous faces or motion illusion that selectively involved the fusiform gyrus[42] and premotor areas[44], respectively. This response pattern was considered to support the involvement of sensory and predictive mechanisms in integrating contextual information to resolve visual ambiguity[44].

These findings do not seem to support the engagement of affect- and/or reward-related brain responses when processing visual ambiguity in non-artistic[42] or artistic[31] contexts. However, this conclusion is in striking conflict with behavioural evidence from studies entailing the analysis of ambiguous artworks[27,47]. Indeed, their results rather highlighted the role played by the motivation and reward associated with processing and trying to solve visual ambiguity, which is reported as stimulating and challenging[27,33]. A dynamic gain of insights seems to represent the critical factor enhancing the reward inherent in the challenging—and therefore stimulating—analysis of visual ambiguity in artistic stimuli[33]. Interestingly, the experience of this feeling even when participants are not fully able to solve such ambiguity suggests that the associated reward might reflect the challenging processing even more than its successful completion[27,48].

On this ground, the present study aims to investigate both the behavioural processes of visual exploration and aesthetic appreciation, and the underlying neural patterns of brain activity and connectivity, while processing visual ambiguity in challenging and stimulating artworks. To this purpose, *f*MRI was combined with eye-tracking - to measure both brain activity and the number of fixations (a reliable metric of intensive interest for a given stimulus;[49])—in participants presented with ambiguous or non-ambiguous photographs differing with respect to the presence of multiple potential interpretations. Based on the notion of street photography as a mature form of art[50], we took advantage of the potential of photographic artistic stimuli in terms of the precise characterization and balance of multiple semantic dimensions across ambiguous and non-ambiguous photographs[51]. In particular, to ensure that brain activity was driven by our manipulation of visual ambiguity rather than the appreciation of the artwork itself, we balanced ambiguous and non-ambiguous stimulus types for aesthetic appreciation based on the results of a preliminary rating procedure. We predicted that - also in the case of photographic aesthetics - the processing of ambiguous (compared with non-ambiguous) artistic stimuli would recruit fronto-parietal and occipito-temporal areas underlying the computational facets of processing and solving visual ambiguity[37,44], alongside structures supporting the reward inherent in developing insights about their artistic meaning[27].

Materials and methods

Participants

34 right-handed healthy volunteers (25 females and 9 males; mean age = 22.9 years, standard deviation (SD) = 3.8, range = 19–39) participated in the study. To ensure high data quality, as described below (see sections "Analysis of eye-tracking data" and "fMRI data preprocessing") we removed from statistics 11 participants exceeding pre-defined thresholds of scan-to-scan head motion ($n = 5$) or broken visual fixations during stimulus presentation ($n = 6$). The final sample therefore included 23 right-handed healthy volunteers (18 females and 5 males; mean age = 22.6 years, standard deviation (SD) = 2.9, range = 19–29). All participants had normal or corrected-to-normal visual acuity. None of them reported a history of neuro-psychiatric conditions or substance abuse, nor was currently taking any medication interfering with cognitive functioning. They gave their written informed

consent to the experimental procedure, that was approved by the Ethics Committee of IRCCS Ospedale San Raffaele (Milan, Italy) and performed in accordance with the Declaration of Helsinki.

Stimuli and task

Participants were presented with colour photographs of various kinds of indoor and outdoor sceneries, classified into two distinct experimental conditions differing for stimulus type, i.e., with (AMB+) and without (AMB-) graphical elements generating visual ambiguity and multiple possible interpretations (see Fig. 1).

AMB + photographs were characterized by the presence of natural visual reflection (e.g., reflections from mirrors, water, glasses, etc.), that resulted in natural visual ambiguity, i.e., difficulty in understanding which part of the image is real and which is reflected. AMB- photographs served as baseline, to isolate neural responses underlying the processing of visual ambiguity in aesthetic photography while controlling for the analysis of semantic visual features, as well as for motor responses and their preparation. AMB– stimuli were searched and selected from Google image database so as to balance the presence of objective semantic features (other than the elements generating visual ambiguity) that might confound the interpretation of behavioural and neural findings, such as the presence of biological stimuli and other relevant semantic features (see Table 1 for the full list of features taken into consideration). The different properties of AMB + and AMB- photographs were confirmed by 20 participants (13 females and 7 males other than those recruited for the *f*MRI study), who were asked to indicate, for each stimulus, whether it presented a visual reflection (yes/no response). Results indeed showed that AMB + images were more strongly characterized by visual reflection (AMB+: mean response = 0.97, SD = 0.71 AMB–: mean response = 0.26, SD = 0.17; $t(81.42) = 30.14$, $p < 0.001$). These procedures resulted in a final selection of 62 AMB + and 62 AMB- photographs.

The retained stimuli underwent a preliminary rating procedure, with 60 participants (45 females and 15 males other than those recruited for the *f*MRI study and for the first assessment on visual reflection) who were asked to evaluate—on a 7-level scale—the degree to which they considered each photograph to be (a) complex, (b) beautiful, and (c) stimulating (20 raters per dimension). AMB + photographs were rated as more complex ($t(122) = 11.33$, $p < 0.001$) and stimulating ($t(122) = 2.35$, $p = 0.020$) than AMB- ones, with no significant difference concerning beauty ($t(122) = 0.49$, $p = 0.62$). This procedure therefore ruled out the possibility that any difference in the neural processing of AMB + and AMB- photographs could be attributed to their aesthetic quality per se (see "Introduction").

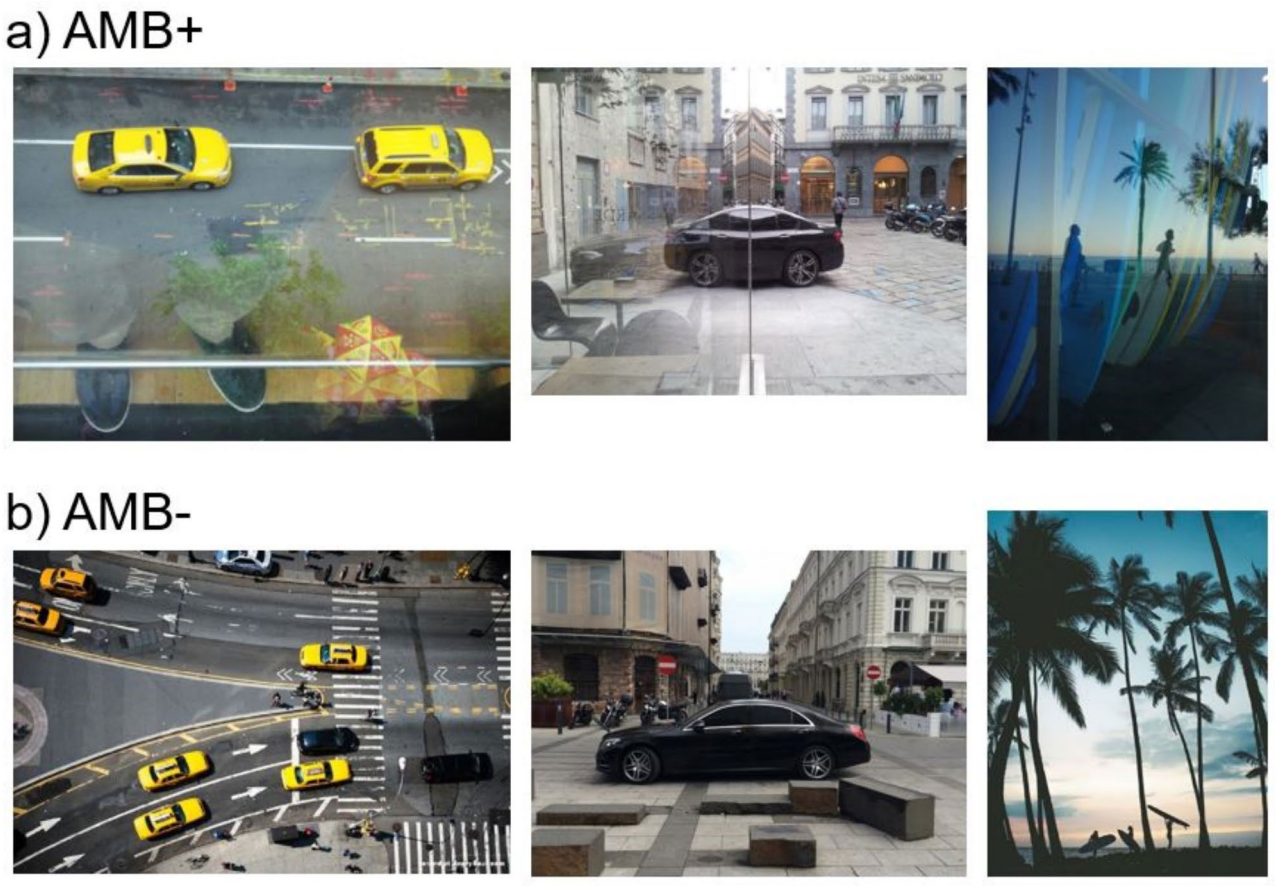

Fig. 1. Stimuli examples. The figure depicts selected examples of ambiguous (AMB+) and unambiguous (AMB–) photographs.

Orientation (vertical vs. horizontal)
Presence of simmetry
Presence of famous places
Pedagogical elements (verbal indications specifying the location)
Presence of biological stimuli
Presence of buildings
Presence of inanimate stimuli as animate (e.g., mannequin)
Presence of food (reward)
Presence of clothes or jewellery or watches (reward)
Time of the day of photo shoot (day vs. evening)
Presence of objects/photos/images depicting human figures
Presence of movements and dynamism
Presence of objects
Presence of manipulable objects
Presence of inscriptions
Presence of branded inscriptions
Presence of animals
Presence of vegetation
Presence of art stimuli

Table 1. Full list of features considered in stimuli selection. The table reports the full list of features that were balanced across AMB + and AMB– photographs.

During *f*MRI, every stimulus was presented once for each of two experimental tasks, in which participants were either asked to (a) just watch the photograph as if they were attending a photo exhibition (Watch Only, i.e., WO); or (b) watch the photograph while preparing to evaluate - on a 4-level scale - how beautiful they experienced them to be (not at all, a little, much and very much) (Watch-Evaluate, i.e., WE). To enable an implicit aesthetic processing of stimuli in the WO task, the latter always preceded the WE task during *f*MRI (see "Experimental design and procedures"), and participants were informed of the additional WE requirements only at the beginning of the corresponding *f*MRI runs. Importantly, the fact that the same photographs were presented in both tasks without counterbalancing their order does not allow to exclude that any evaluation-specific activation might be biased by repetition effects, and therefore represents an inherent limitation of the present experimental design. In keeping with previous related studies (e.g.,[3]), however, this design was aimed at enabling a passive observation of stimuli that would have been prevented by the previous request to evaluate them.

Experimental design and procedures

Participants read standardized instructions and underwent a training session before *f*MRI scanning. The whole experiment included 2 WO runs (62 photographs per run, corresponding to 10 min 37 s) followed by 4 WE runs (31 photographs per run, corresponding to 7 min 1 s). Each run started with written instructions, lasting 4 s. Every stimulus was presented once for each of the two experimental tasks. Photographs were shown for 5 s both in the WO and WE tasks. In the latter, each stimulus was followed by a blank screen (lasting 4 s) and a screen (lasting 2.5 s) depicting the four possible aesthetic evaluations (from left to right: not at all, a little, much and very much). Participants were instructed to provide their assessment of each photograph after the onset of this screen, by pressing, with the four fingers (index to pinkie) of the right hand, one of four buttons on an MRI-compatible response-box, corresponding to the left-right spatial locations of the four possible responses.

To optimize our design and detect the overlapping hemodynamic responses to stimuli closely spaced in time, the duration of interstimulus intervals (ISIs) were varied across trials[51]. To this purpose, successive trials were separated by ISIs, during which a white fixation-cross was shown, which were presented in different ("jittered") durations across trials (mean = 5200 ms; range = 2000–16800 ms).

Presentation software (v23.1; http://www.neurobs.com) was used both to collect responses through a 4-button fiber optic response box (Current Designs, Philadelphia, PA), and to deliver stimuli via *f*MRI-compatible binocular OLED video goggles (Nordic Neurolab VisualSystem, Bergen, Norway) that were mounted to the head-coil and oriented toward both eyes. This visual presentation system, providing 800 × 600-pixel resolution with a field-of-view that nominally spans 23.5° in the vertical direction and 30° in the horizontal direction, was also used to record eye position binocularly at 60 Hz - during the whole scanning session - through an infrared video eye-tracker. Before each *f*MRI run, the eye-tracker was calibrated at a central position and at 8 eccentric points. During each run, changes in pupil position in the horizontal (X) and vertical (Y) directions were computed online and sampled at 60 Hz using the image-analysis software ViewPoint® (v2.9.5; http://www.arringtonresearch.com/viewpoint.html) that is integrated with the visual presentation/eye-tracking hardware. The resulting eye-tracking data were recorded from both eyes and saved separately for offline analysis.

fMRI data acquisition

We collected anatomical T1-weighted and functional T2*-weighted MRI images with a 3 Tesla Philips Ingenia CX scanner (Philips Medical Systems; Best, The Netherland), equipped with a 32-channels head coil. Participants were positioned comfortably on the scanner bed and fitted with soft ear plugs; foam pads were used to minimize head movements. Functional images were acquired using an echo-planar-imaging (EPI) sequence with multiband factor = 2 (52 interleaved ascending transverse slices covering the whole brain, tilted 30° downwards with respect to the bicommissural line to reduce susceptibility artifacts in orbitofrontal and inferior temporal regions; TR = 1400 ms, TE = 30 ms, flip-angle = 85°, field-of-view (FOV) = 192 mm × 192 mm, no interslice gap, in-plane resolution = 3 mm × 3 mm, slice thickness = 3 mm), preceded by 5 "dummy" functional volumes covering the amount of time required for T1-equilibration effects. A high-resolution 3D T1-weighted brain scan was also acquired along the AC-PC plane (243 slices, FOV = 384 × 384 mm, in-plane resolution = 0.7 × 0.7 mm, slice thickness = 0.7 mm).

Analysis of behavioural data

The SPSS software (v. 29.0.1; https://www.ibm.com/it-it/spss) was used to perform paired-sample t-tests assessing possible differences in aesthetic evaluation across AMB + and AMB- photographs during *f*MRI scanning. The Kolmogorov-Smirnov test confirmed that the normality assumption was met.

Analysis of eye-tracking data

Eye movement data were collected using Viewpoint® software, which recorded raw eye movement signals at a sampling rate of 60 Hz, along with operational events, generating logfiles. Viewpoint® logfiles were then imported into Matlab (v9.13.0 (R2022b); https://www.mathworks.com/products/matlab.html) for preprocessing and analysis of the raw eye-tracking signals. Visual fixation events were identified through an adaptive algorithm using a data-driven adaptive velocity threshold that dynamically adjusts to accommodate different viewers, recording conditions, and noise levels across the entire experiment or individual trials[52].

This procedure allowed to quantify the number of fixations for each participant, task (WO, WE) and stimulus type (AMB+, AMB–). We used a Generalized Linear Mixed Model (GLMM) to assess whether the number of fixations was significantly modulated by stimulus type (AMB + vs. AMB– photographs) and task (WO vs. WE), or their interaction, during *f*MRI scanning.

From a physiological perspective, it must be noted that fixations are essential for visual perception[53], and, accordingly, the absence of fixations during the 5-second presentation of a photograph indicates either inadequate engagement in the task, or a failure of the eye-tracking device to accurately detect and track the pupil movements. Consequently, to ensure high-quality data, 6 participants with 0 fixations for more than 50% of the stimuli (AMB+, AMB-) within each task (WO, WE) were excluded from analyses (see Supplementary Table 1 for details on the number of fixations for each participant and experimental factor).

fMRI data preprocessing

We performed the pre-processing and statistical analyses of *f*MRI data using SPM12 (http://www.fil.ion.ucl.ac.uk/spm), implemented in Matlab (v9.11 (R2021b); https://www.mathworks.com/products/matlab.html)[54]. The 2114 volumes from each subject underwent a standard spatial preprocessing including slice-timing correction with the middle slice in time as reference, spatial realignment to the first volume and unwarping, spatial normalization into the standard Montreal Neurological Institute (MNI) space, as well as spatial smoothing with a 8 mm full-width half-maximum (FWHM) isotropic Gaussian kernel. The resulting timeseries across each voxel were then high-pass filtered to 1/128 Hz, and serial autocorrelations were modelled as an autoregressive AR(1) process. We used the MotionFingerprint toolbox (v.1.6.2; http://www.medizin.uni-tuebingen.de/kinder/en/research/neuroimaging/software/)[55] to compute a comprehensive indicator of total and framewise (i.e., scan-to-scan) head motion for each subject. A pre-specified threshold of average framewise displacement < 0.15 mm led to remove 5 further participants. The average total displacement in the final sample of 23 participants was 0.563 ± 0.182 mm, while the average framewise displacement was 0.068 ± 0.015 mm.

Analysis of brain activity

Statistical analyses were aimed at isolating the voxels showing a significant effect of stimulus type (AMB + vs. AMB-), task (WO vs. WE), or their interaction, on brain activity associated with (a) task execution, (b) aesthetic appreciation based on participant's rating (henceforth, "beauty-related activity"), or (c) number of fixations based on eye-tracking data (henceforth, "fixation-related activity"). We pursued this goal via a random-effect model implemented in a two-levels procedure[56].

At the first (single-subject) level we modelled *f*MRI responses as mini-epochs in a design-matrix comprising the onset of all stimuli for each of the 4 conditions of interest (i.e., WO/AMB+, WO/AMB–, WE/AMB+, WE/AMB–) with duration = 5 s. The design matrix additionally included the rating epoch in WE task (duration = 2.5 s), and a single regressor of no interest encoding the onset of both the instructions and the whole WE trials that were removed due to lack of responses.

Each of the 4 condition-specific regressors was associated with a parametric regressor coding a trial-wise linear modulation of task-related activity by (a) participant's evaluation, and (b) number of fixations. For WO trials, stimulus-wise evaluation values corresponded to those provided to the same photographs in the WE task. To increase statistical power in subsequent connectivity analyses, we concatenated the 6 functional runs to form one single timeseries per subject, and added a regressor modelling session effects. A regressor coding framewise displacement was also included in the model. We then convolved regressors modelling events with a canonical hemodynamic response function (HRF), and we obtained parameter estimates for all regressors by maximum-likelihood estimation. The resulting first-level beta maps were contrasted to highlight the voxels in

which significant changes of activity reflected either (a) each of the four conditions, regardless of evaluation or number of fixations; (b) condition-specific evaluation, regardless of the number of fixations; (c) condition-specific number of fixations, regardless of evaluation.

The resulting single-subject contrast images were entered into distinct group-level analyses aimed to unveil the voxels in which these 3 dependent variables of brain response reflected the effect of task (WO/WE), stimulus type (AMB+/AMB-), or their interaction, via a 2 (WO/WE) x 2 (AMB+/AMB–) factorial design.

The resulting SPMs were thresholded at $p < 0.05$ corrected for multiple comparisons based on cluster-extent using topological false discovery rate (FDR;[57]), with $p < 0.001$ at the voxel-level. To ensure the robustness of our results we also used probabilistic threshold-free cluster enhancement (pTFCE; v0.2.0; https://spisakt.github.io/pTFCE/)[58], that integrates cluster information into voxel-wise statistical inference (see[59]).

We used the SPM Anatomy Toolbox (v.2.2c; https://www.fil.ion.ucl.ac.uk/spm/ext/)[60] to localize the activated brain regions in the MNI space in terms of (a) microanatomical labels based on the overlap between each cluster and probabilistic cytoarchitectonic maps (when available); (b) macroanatomical labels provided by the Automated Anatomical Labeling (AAL3; https://www.fil.ion.ucl.ac.uk/spm/ext/) atlas[61,62] for clusters located outside these maps.

Analysis of brain connectivity

*f*MRI results informed a subsequent Psycho-PhysiologicaI-Interaction (PPI) analysis[63] aimed to unveil the functional neural interactions underlying the interactive effect of task (WO/WE) and stimulus type (AMB+/AMB-) on brain activity.

The PPI approach highlights a significant increase/decrease of connectivity, from a seed region to all other brain voxels, in association with a given context, by regressing the activity at any voxel on the activity of the seed. PPI represents an advancement with respect to functional connectivity analyses based on pairwise temporal correlation, which cannot disambiguate context-specific connectivity from resting-state connectivity or connectivity associated with a common neuro-modulatory input. Indeed, to discount correlations due to shared task inputs, the PPI model also includes—as nuisance covariates—the activity of the seed region and an experimental context, i.e., the physiological and psychological factors, respectively. The resulting regression coefficient represents, at every voxel, the degree of change in activity per unit change in the seed region, or in simpler words a measure of the influence one neural system has on another, due to a psychological variable that—based on *f*MRI results (section "Fixation-related brain activity")—was here represented by the number of fixations when processing photographs. In keeping with our aim and hypotheses (see "Introduction"), we therefore investigated changes of connectivity, reflecting the interactive effect of task and stimulus type on brain activity tracking the number of fixations, between the left medial prefrontal cortex cluster showing the same interaction in standard *f*MRI analyses (section "Fixation-related brain activity") and any other brain voxel.

PPI analyses were carried out with the CONN toolbox (v22a; https://web.conn-toolbox.org/). *F*MRI timeseries first underwent denoising steps aimed to remove the effects of non-neural noise related to linear drifts in the BOLD signal, subject-specific head motion, and physiological noise related to cardiac and respiratory sources, through the "anatomical component-based noise correction" (aCompCorr) method[64], as previously reported[65].

We then defined our region-of-interest (ROI) as a 8-mm radius sphere centred on the peak coordinates of the left medial prefrontal cortex cluster that, in standard *f*MRI analyses, was found to reflect the same interactive effect of task and stimulus type on brain activity tracking the number of fixations (see section "Fixation-related brain activity"). The first eigenvariate of the BOLD timeseries from this ROI was then extracted, temporally filtered, mean corrected and deconvolved to generate the underlying neuronal signal. We then created: (a) the interaction factor (PPI regressor), i.e., the product of the mean-centred task time course and the demeaned seed ROI time course; (b) the psychological factor (P regressor) representing the contrast for fixation-related activity in the single conditions; and (c) the physiological factor (Y regressor) representing the ROI time course. These regressors were convolved with the canonical hemodynamic response function (HRF), and entered into a regression model also including regressors for framewise head displacement and session effects. This procedure was carried out for each subject, and the resulting images of contrast estimates were entered into a random-effect group analysis to isolate voxels in which significant changes of connectivity with the seed region reflected the interactive effect of task (WO/WE) and stimulus type (AMB+/AMB-) on fixation-related activity.

The resulting group-level maps were thresholded at $p < 0.05$ FDR corrected based on cluster-extent (forming threshold: $p < 0.001$ uncorrected at the voxel-level).

Results

Behavioural results

Participants' assessment on the WE task showed no significant difference between AMB + and AMB- photographs in terms of aesthetic appreciation (Table 2). GLMM results highlighted a significantly larger number of fixations in the WE, compared with WO, task (Table 2). Instead, there was neither a modulation by stimulus type nor an interaction between task and stimulus type (Table 2) on the number of fixations.

fMRI results

Brain activity related to task or stimulus type

Regardless of stimulus type, WO, compared with WE, task recruited a widespread set of areas encompassing the left middle occipital cortex and the cerebellum, the middle temporal gyrus (MTG) extending to the amygdala and hippocampus bilaterally, as well as the anterior cingulate cortex (ACC) bilaterally (Table 3; Fig. 2a), likely supporting a spontaneous affective processing of the aesthetic qualities of attended stimuli (see "Discussion", and Supplementary Fig. 1 for group-level histograms depicting mean activity and 90% confidence intervals for these regions).

Metric	Contrast	Estimate	SE	df	t-value	*p*-value
Aesthetic appreciation	AMB + vs. AMB–	0.015	0.023	22	0.75	0.45
Number of fixations	WE vs. WO	0.088	0.018	4934	4.853	< 0.0001
Number of fixations	AMB + vs. AMB-	-0.010	0.019	4934	0.553	0.580
Number of fixations	Interaction "task" x "stimulus type"	0.009	0.026	4934	0.368	0.713

Table 2. Behavioural results. From left to right, the table reports the statistical values for the main contrasts and variables of interest.

Cluster size	Hem	Anatomical region	x	y	z	t-value
1599	R	Hippocampus	38	– 36	– 10	5.49
	R	Amygdala	36	4	– 26	5.04
	R	Middle Temporal Gyrus	50	– 6	– 18	4.7
	R	Temporal Pole	50	8	– 30	3.93
	R	ParaHippocampal Gyrus/Hippocampus	20	– 10	– 24	3.58
1568	L	Hippocampus	– 36	– 24	– 12	5.78
	L	Fusiform Gyrus	– 38	– 10	– 24	4.86
	L	Amygdala	– 28	2	– 22	4.35
	L	Middle Temporal Gyrus	– 48	– 10	– 20	4.23
	L	Cerebellum (Lobule IV-V)	– 22	– 32	– 28	3.55
553	R	Ventral ACC (subgenual cortex)	4	22	– 8	4.85
	L	Ventral ACC (subgenual cortex)	– 10	34	– 8	4.37
	L	Middle Orbital Gyrus	– 12	38	– 8	3.89
416	L	Middle Occipital Gyrus	– 42	– 68	24	5.64
374	R	Superior Parietal Lobule	14	– 54	62	4.53

Table 3. Stronger brain activity when observing, compared with evaluating, stimuli. From left to right, the table reports the extent (number of $2 \times 2 \times 2$ mm^3 voxels), hemispheric lateralization (Left/Right), anatomical labeling, stereotactic coordinates and statistical value for the clusters showing a stronger response when performing WO than WE task ($p < 0.05$ FWE corrected). Hem: Hemisphere; ACC: Anterior Cingulate Cortex.

Instead, the opposite comparison highlighted the engagement of left-hemispheric structures that have been associated with attentional and executive processes[3,66,67], such as the inferior frontal (IFG) and precentral gyri, the inferior parietal lobule (IPL), the insula and the pallidum, alongside the ACC (extending to the middle cingulate cortex (MCC) bilaterally), plus the right cerebellum (Table 4; Fig. 2b).

When focusing on stimulus type, we found that processing AMB+, compared with AMB-, photographs recruited the middle occipital cortex bilaterally, extending to superior and inferior parietal areas in the right hemisphere, as well as the right IFG (Table 5; Fig. 2c), likely supporting the processing and resolution of visual ambiguity in visual artistic stimuli[44] (see Supplementary Fig. 2 for group-level histograms depicting mean activity and 90% confidence intervals for these regions).

Conversely, AMB-stimuli, compared with AMB + ones, activated the key nodes of the Default Mode Network[68], including both the left lateral fronto-temporal cortex, extending to the anterior insula and medial temporal pole, the frontomedial cortex, involving both the ACC and the medial superior frontal gyrus, the left posterior MTG, supramarginal gyrus and posterior insular cortex, plus the cerebellum bilaterally (Table 6; Fig. 2d). No significant interaction between task and stimulus type were observed.

Evaluation-related brain activity

Regardless of stimulus type, higher *implicit* aesthetic appreciation (in the WO, as compared with WE, task) was linearly and positively related to the strength of occipital activity in the left lingual gyrus (Table 7; Fig. 3a) (see Supplementary Fig. 3 for group-level histograms depicting mean activity and 90% confidence intervals).

In contrast, *explicit* aesthetic appreciation (in the WE, as compared with WO, task) was related to stronger occipital activity in the right lingual and calcarine gyri (Table 8; Fig. 3b). As expected, the lack of significant differences in the aesthetic appreciation of AMB + and AMB- photographs reflected in no significant main effect of stimulus type, or interaction between task and stimulus type, on brain activity.

Fixation-related brain activity

Task-by-stimulus type interaction analyses showed that the activity of the left medial prefrontal cortex (ACC and superior frontal gyrus) was more strongly related to the number of fixations when evaluating (vs. observing) ambiguous (vs. non-ambiguous) photographs (Table 9; Fig. 3c) (see Supplementary Fig. 3 for group-level histograms depicting mean activity and 90% confidence intervals). In particular, we observed a significant linear positive correlation between brain activity and number of fixations only when evaluating ambiguous

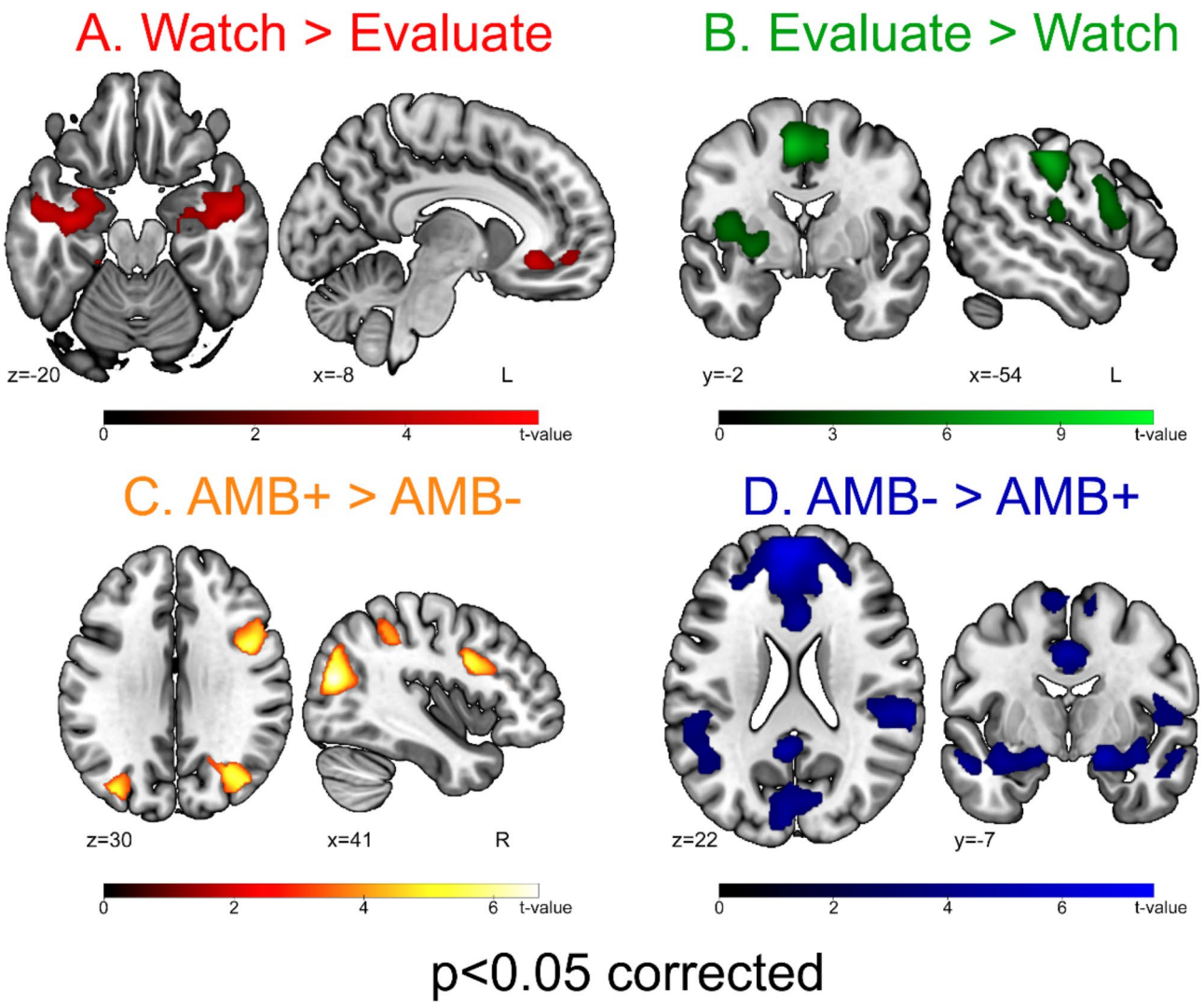

Fig. 2. Task-related brain activity. The figure shows the regions that were more strongly activated by observing than evaluating (A; red) or evaluating than observing (B; green) regardless of stimulus type, as well as by ambiguous than non-ambiguous (C; yellow) or non-ambiguous than ambiguous (D; blue) photographs regardless of task ($p < 0.05$ corrected). Colorbars depict the range of t-values reported in each figure panel, with brightest colors reflecting highest t-values and, accordingly, strongest brain activity.

photographs ($r = 0.583$, $p = 0.0035$), while this correlation was not significant in the other three conditions (observing-ambiguous: $r = -0.350$, $p = 0.101$; observing-non ambiguous: $r = 0.104$, $p = 0.637$; evaluating-non ambiguous: $r = -0.151$, $p = 0.502$). No other significant main effects of tasks or stimulus type were observed. The available evidence suggests that the engagement of this region might reflect the depth of visual exploration, promoting the encoding and integration of multiple features as an essential mean to resolve visual ambiguity[69]; see "Discussion").

Fixation-related functional connectivity

A PPI connectivity analysis was performed to investigate trial-wise changes of functional connectivity, reflecting the interactive effect of task and stimulus type on fixation-related brain activity, between the left medial prefrontal cluster showing the same interaction in standard *f*MRI analyses (section "Fixation-related brain activity") and any other brain voxel. The larger number of fixations when watching to evaluate (WE), compared with only watching (WO), therefore represents a reference for interpreting the present PPI results in terms of increased or decreased seed-to-voxel connectivity. Under this assumption, the number of fixations associated with watching to evaluate (compared with just observing) AMB+ (compared with AMB-) photographs, reflected in decreased connectivity from the left medial prefrontal cortex (x=-12, y = 48, z = 4) to its homologue region in the right hemisphere (x = 14, y = 54, z = 30) (Fig. 3d; Table 10). Based on previous related findings, this interhemispheric prefrontal inhibitory connectivity might support in-depth visuospatial analyses aimed to evaluate, and make sense of, artistic ambiguous stimuli[70]; see "Discussion").

Cluster size	Hem	Anatomical region	x	y	z	t-value
2812	L	Precentral Gyrus	− 32	− 24	56	11.5
	L	Inferior Parietal Lobule	− 50	− 26	44	8.49
	L	Rolandic Operculum	− 46	− 22	18	6.26
2419	L	Posterior Frontal Gyrus	− 6	− 4	52	8.53
	L	MCC	− 6	20	38	5.53
	L	ACC	− 8	28	30	5.04
	R	MCC	8	28	30	4.62
1248	L	IFG (pars Opercularis)	− 56	8	22	5.98
	L	Pallidum	− 26	− 8	− 2	5.21
	L	Rolandic Operculum	− 40	− 4	14	4.95
	L	Insula Lobe	− 32	16	8	4.8
772	L	Middle Frontal Gyrus	− 30	46	20	5.21
	L	IFG (pars Triangularis)	− 34	34	24	4.79
529	R	Cerebellum (Lobule IV-V)	18	− 52	− 22	8.49

Table 4. Stronger brain activity when evaluating, compared with observing, stimuli. From left to right, the table reports the extent (number of $2 \times 2 \times 2$ mm^3 voxels), hemispheric lateralization (Left/Right), anatomical labeling, stereotactic coordinates and statistical value for the clusters showing a stronger response when performing WE than WO task. Hem: Hemisphere; MCC: Middle Cingulate Cortex; ACC: Anterior Cingulate Cortex; IFG: Inferior Frontal Gyrus.

Cluster size	Hem	Anatomical region	x	y	z	t-value
1972	R	Middle Occipital Gyrus	42	− 74	18	6.73
	R	Intraparietal Solcus	28	− 58	40	5.99
	R	Inferior Parietal Lobule	34	− 46	46	5.15
	R	Superior Parietal Lobule	18	− 68	54	4.25
	R	Precuneus	20	− 56	22	3.71
582	R	IFG (pars Opercularis)	44	8	28	5.76
436	L	Middle Occipital Gyrus	− 36	− 80	28	5.52

Table 5. Stronger brain activity when processing AMB+, compared with AMB-, stimuli. From left to right, the table reports the extent (number of $2 \times 2 \times 2$ mm3 voxels), hemispheric lateralization (Left/Right), anatomical labeling, stereotactic coordinates and statistical value for the clusters showing a stronger response to AMB + than AMB- photographs. Hem: Hemisphere; IFG: Inferior Frontal Gyrus.

Discussion

While visual ambiguity is known to play a central role in modern art[71], contributing to make artworks more challenging and stimulating[26], the neural correlates underlying its processing have been only marginally studied by the rising field of Neuroesthetics. To fill this gap, we combined *f*MRI with eye-tracking to investigate the visual and neural processing of the multiple potential interpretations of ambiguous (AMB+) vs. non-ambiguous (AMB-) photographs ("stimulus type" factor) that were either evaluated (WE) vs. just watched (WO) ("task" factor) by 23 healthy young participants.

The latter experimental manipulation showed that—regardless of stimulus type—evaluating (WE task) the photographs, as compared with just observing them (WO task), was associated both with a larger number of visual fixations, and with stronger activity in the left (IFG) and precentral gyrus, extending into the anterior insula, alongside the IPL. Instead, the opposite comparison highlighted the involvement of a widespread set of structures encompassing the bilateral MTG, extending to the amygdala, the fusiform gyrus, and the cerebellum. This functional segregation fits with previous evidence indicating that evaluating and passively observing are cognitively different tasks engaging alternative strategies and distinct neural mechanisms[67,72]. Providing an explicit judgment is indeed expected to entail a stronger loading on attentional and executive processes, in turn likely decreasing the spontaneous emotional neural response to aesthetic stimuli[3,67]. In keeping with this hypothesis, we found that evaluating, as compared with observing, stimuli was associated with a stronger recruitment of the left inferior frontal and parietal cortex. Based on task requirements, these activations might be suggestive of a stronger engagement of the ventral attentional network underlying the reorienting of spatial attention[73] when evaluating stimuli, whereas just observing them engaged brain structures that might collectively underpin a more spontaneous affective processing of their aesthetic qualities. It is worth noting that the ventral attentional network is usually considered to be lateralized in the right hemisphere[74–76], but this view has been questioned by neuroimaging and neurostimulation studies[77]. Moreover, in keeping with previous proposals on the contribution of multimodal integration—driven by the cortical motor system—to the aesthetic

Cluster size	Hem	Anatomical region	x	y	z	t-value
10,956	L/R	Superior Medial Gyrus	0	58	16	7.62
	L	ACC	− 10	46	− 4	7.07
	R	Superior Frontal Gyrus	18	40	34	6.32
	R	ACC	12	46	12	6.29
7967	L	Insula Lobe	− 26	16	− 16	5.84
	R	Amygdala	20	− 2	− 18	5.73
	L	Middle Temporal Gyrus	− 42	6	− 32	5.66
	L	IFG (pars Orbitalis)	− 44	26	− 10	5.53
	R	Superior Temporal Gyrus	52	− 32	12	5.43
	R	SupraMarginal Gyrus	64	− 32	24	5.23
	L	Hippocampus	− 22	− 28	− 6	4.99
	L	Caudate Nucleus	− 4	14	− 6	4.83
	R	Temporal Pole	36	4	− 34	4.72
4821	L	Calcarine Gyrus	− 8	− 80	6	5.68
	R	Lingual Gyrus	8	− 62	0	5.66
	R	Calcarine Gyrus	14	− 72	8	5.33
	L	Superior Occipital Gyrus	− 8	− 96	8	4.92
	L	Cuneus	− 4	− 84	16	4.72
	L	Middle Occipital Gyrus	− 18	− 98	10	4.26
1137	R	Cerebellum (Crus 1)	28	− 76	− 34	5.6
	R	Cerebellum (VII)	40	− 52	− 44	4.26
	R	Cerebellum (VI)	30	− 56	− 28	3.56
717	L	Cerebellum (Crus 2)	− 28	− 84	− 31	4.82
	L	Cerebellum (Crus 1)	− 40	− 60	− 33	4.43
	L	Cerebellum (VI)	− 28	− 56	− 29	4.16
	L	Cerebellum (VIII)	− 30	− 62	− 45	3.86
665	L	Insula Lobe	− 34	− 30	20	4.26
	L	Angular Gyrus	− 48	− 62	26	4.06
	L	Superior Temporal Gyrus	− 54	− 34	18	3.89
396	L	PCC	− 4	− 54	31	5.31

Table 6. Stronger brain activity when processing AMB-, compared with AMB+, stimuli. From left to right, the table reports the extent (number of 2 × 2 × 2 mm3 voxels), hemispheric lateralization (Left/Right), anatomical labeling, stereotactic coordinates and statistical value for the clusters showing a stronger response to AMB- than AMB + photographs. Hem: Hemisphere; ACC: Anterior Cingulate Cortex; IFG: Inferior Frontal Gyrus; PCC: Posterior Cingulate Cortex.

Cluster size	Hem	Anatomical region	x	y	z	t-value
485	L	Lingual Gyrus	-12	− 68	− 6	5.92

Table 7. Evaluation-related brain activity when observing, compared with evaluating, stimuli. From left to right, the table reports the extent (number of 2 × 2 × 2 mm3 voxels), hemispheric lateralization (Left/Right), anatomical labeling, stereotactic coordinates and statistical value for the cluster showing a stronger relationship with (implicit) beauty assessment during WO compared with WE task. Hem: Hemisphere.

experience[8,78,79], the attentional reorienting required by evaluating, rather than just observing, artistic stimuli might involve the output of "simulation" processes associated with the left-hemispheric inferior frontal and inferior parietal nodes of the mirror network[80–82].

The possible differences across evaluating and passively observing were also investigated with respect to the individual trial-wise appreciation, as encoded by the linear parametric modulation of task-related activity by aesthetic judgment. To this purpose, we compared the parametric neural effect of one's own aesthetic appreciation across the WE task (in which judgments were explicitly provided) and the WO one (in which no judgment was given, and the evaluation values corresponded to those provided to the same photographs in WE). We thereby found lateralized effects of implicit and explicit aesthetic appreciation in left and right occipital regions, respectively. Based on the available relevant literature, this lateralization might have been driven by the prominent role of the left and right occipital cortex in processes closer to the requirements posed by WO and WE

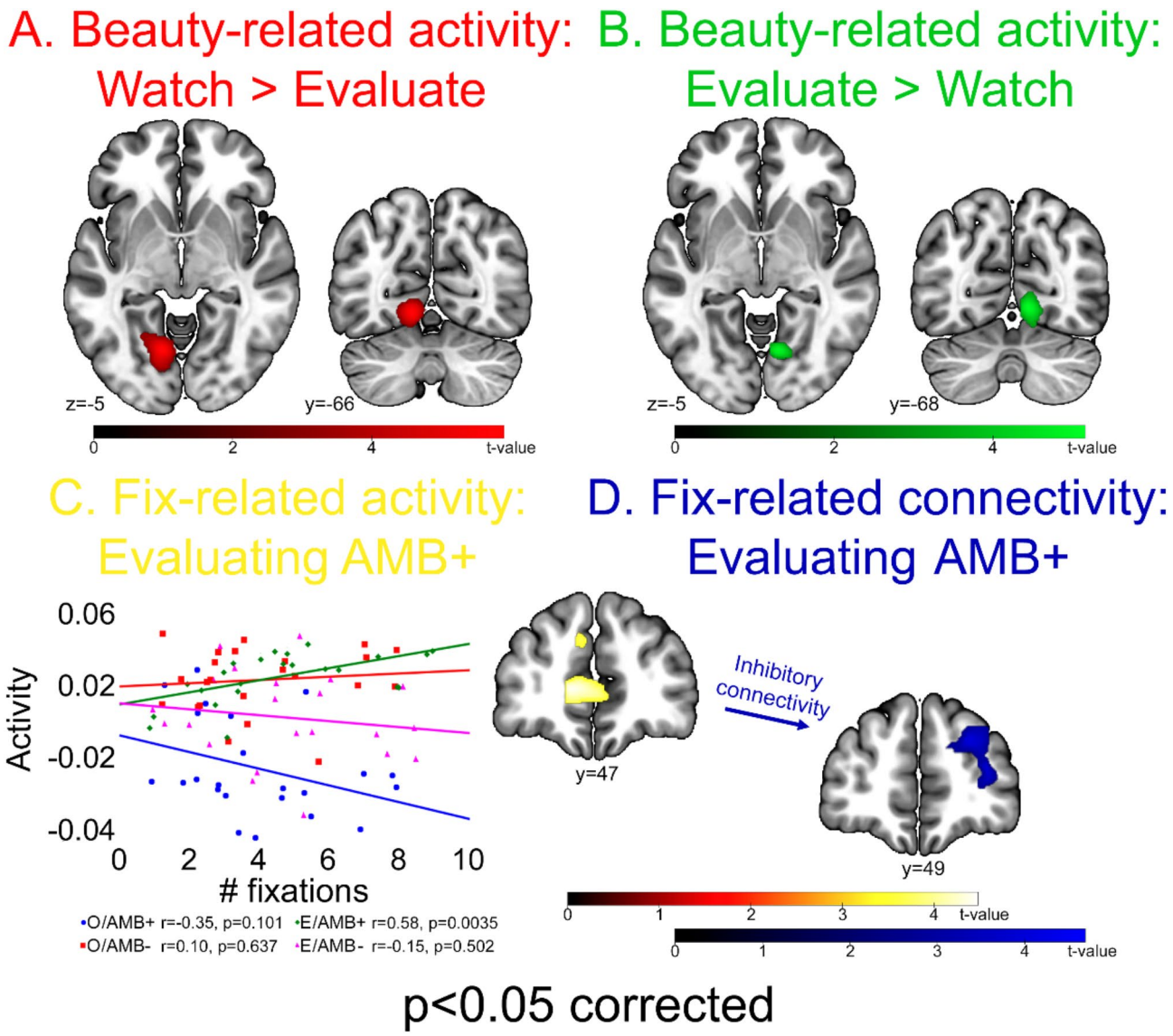

Fig. 3. Evaluation- and fixation-related brain activity and connectivity. The top figure sector depicts the regions showing a stronger relationship with (implicit) beauty assessment during WO compared with WE task (A; red) or with (explicit) beauty assessment during WE compared with WO task (B; green). The bottom figure sector depicts the left medial prefrontal cluster showing stronger fixation-related activity when evaluating (vs. observing) ambiguous (vs. non-ambiguous) photographs (interaction analysis) (C; yellow) alongside the scatterplot of activity against the number of fixations in the four conditions, as well its right-hemispheric target of decreased connectivity in the same condition (evaluating ambiguous photographs; D; blue). Colorbars depict the range of t-values reported in each figure panel, with brightest colors reflecting highest t-values and, accordingly, strongest brain activity.

tasks, such as natural and intrinsic visual exploration[83] vs. active visuo-spatial exploration of the stimuli[42,84–86], respectively.

Our main goal was to investigate the effect of visual ambiguity on the neural processing of aesthetic photographic stimuli, by comparing brain activations associated with AMB + and AMB- photographs. Regardless of task, processing ambiguous, compared with non-ambiguous, stimuli recruited an extensive network involving fronto-parietal and occipito-temporal areas. These activations were more extensive in the right hemisphere, and, in particular, the right superior parietal lobule (SPL) was selectively recruited by processing ambiguous photographs. This region is considered a crucial hub for the resolution of visual ambiguity, specifically concerning the (re)orientation of attention to global vs. local aspects[87] and the visuospatial analysis of complex visual image[88]. The latter function is likely supported by the right SPL role as a higher-level processing unit, supporting the formation of visual percepts through information from the occipital cortex[44], which explains its engagement in the processing of illusion[44,89], as well as in action preparation via fronto-parietal interactions[90–93]. The present evidence fits with previous reports of the SPL engagement during the evaluation of ambiguous portraits[31], that is

Cluster size	Hem	Anatomical region	x	y	z	t-value
295	R	Lingual Gyrus	10	− 68	− 2	5.2
	R	Calcarine Gyrus	14	− 74	6	4.21

Table 8. Evaluation-related brain activity when evaluating, compared with observing, stimuli. From left to right, the table reports the extent (number of 2 × 2 × 2 mm3 voxels), hemispheric lateralization (Left/Right), anatomical labeling, stereotactic coordinates and statistical value for the cluster showing a significantly stronger relationship with (explicit) beauty assessment during WE compared with WO task. Hem: Hemisphere.

Cluster size	Hem	Anatomical region	x	y	z	t-value
496	L	Medial superior frontal gyrus	− 12	48	4	4.05
	L	ACC	− 4	44	− 2	3.59

Table 9. Fixation-related brain activity: "task-by stimulus type" interaction. From left to right, the table reports the extent (number of 2 × 2 × 2 mm3 voxels), hemispheric lateralization (Left/Right), anatomical labeling, stereotactic coordinates and statistical value for the cluster showing stronger fixation-related activity when evaluating (vs. observing) ambiguous (vs. non-ambiguous) photographs. Hem: Hemisphere; ACC: Anterior Cingulate Cortex.

Cluster size	Hem	Anatomical region	x	y	z	t-value
650	R	Medial superior frontal gyrus	14	54	30	4.80
	R	Middle frontal gyrus	34	52	14	4.28

Table 10. Fixation-related brain connectivity: "task-by stimulus type" interaction. From left to right, the table reports the extent (number of 2 × 2 × 2 mm3 voxels), hemispheric lateralization (Left/Right), anatomical labeling, stereotactic coordinates and statistical value for the cluster showing a significant interaction between stimulus type and task on fixation-related connectivity from the left medial prefrontal seed showing the same effect in *f*MRI analyses. Hem: Hemisphere.

indeed more affected after right, than left, hemispheric lesions[32]. Overall, these findings therefore provide novel insights into a growing literature suggesting that the right parietal cortex supports the processing and resolution of visual ambiguity in artistic stimuli. The opposite comparison showed that processing non-ambiguous (AMB-) photographs, compared with ambiguous (AMB+) ones, recruited the anterior cingulate, medial prefrontal, and middle temporal cortex. All these regions are key nodes of the so-called Default Mode Network (DMN;[68]), i.e., an "intrinsic" large-scale brain network that was originally considered to display decreased and increased activity in association with goal-oriented tasks and wakeful rest (mind-wandering), respectively[94]. However, more recent evidence has refined this view, by highlighting the active and dynamic role of the DMN in integrating external and internal information over time, i.e., as a "sense-making network"[95]. While this hypothesis will require further supporting evidence, the DMN regions might then be more strongly engaged by non-ambiguous, compared with ambiguous, stimuli because - in the absence of conflicting cues - the smoother processing of their features makes it easier to make sense of their meaning.

Importantly, processing visual ambiguity in artistic stimuli did not appear to modulate activity in well-established nodes of the so-called "reward" network[96,97], such as basal ganglia or ventromedial prefrontal cortex, that have been previously reported in association with different drivers of the aesthetic experience such as paintings[98], videogames[99], favorite music[100], and even mathematical formulae[101] (see[102] for an overview on the neural processing of "beauty"). While supporting our selection of ambiguous and non-ambiguous stimuli not differing as to their aesthetic value, this negative evidence suggests that the activity of the reward network is not modulated by "ambiguity", and/or its processing, in itself.

Based on the hypothesis that ambiguity resolution might rather entail a prominent loading on visual exploration, we additionally focused on the trial-wise linear modulation of brain activity by the number of fixations. A task-by-stimulus type interaction analysis showed that the activity of the left medial prefrontal cortex was more strongly related to the number of fixations when evaluating (vs. observing) ambiguous (vs. non-ambiguous) photographs. The available literature provides multiple cues for interpreting this specific functional role. While anatomical connections with visual areas enable this region to support visually guided behavior[103], its involvement has been reported in distinct aspects of visual cognition that might help resolve visual ambiguity, such as controlling spatial attention[104], managing uncertainty during decision-making[105], and visuo-spatial memory[106], which might in turn account for its recruitment in tasks entailing the recognition of visually ambiguous objects[107]. Moreover, this region has been reported as a key hub of insight processing[69], which fits with the observed improvement of creativity and problem-solving abilities after left medial prefrontal stimulation[108,109]. Overall, these data suggest that the engagement of this region when evaluating ambiguous

photographs might reflect the depth of visual exploration, in turn promoting the encoding and integration of multiple features as an essential mean to resolve visual ambiguity.

To ground this hypothesis in a network-level view, the left medial prefrontal cortex associated with evaluating ambiguous photographs was modelled as seed in PPI analyses testing the same task-by-stimulus type interaction analysis. PPI results showed that evaluating ambiguous photographs was specifically associated with decreased connectivity from the left medial prefrontal cortex to its right-hemispheric homologue. Related findings from distinct studies help interpret the possible functional role of this inhibitory mechanism when addressing visual ambiguity. First, a similar deactivation of the right medial prefrontal cortex—encompassing the ACC—has been previously reported in association with the recognition of scene configurations, proportionally to task difficulty[110]. Moreover, the deactivation of this region has been reported when comparing spatial tasks with different tasks not involving spatial exploration[111], and when participants were forced to use distal room cues to navigate to a hidden platform in a virtual environment[112]. Most importantly, the degree of deactivation of this region was found to reflect the quality of visual scene recognition[110], thus establishing a link between the efficacy of such inhibitory mechanism and individual performance. Overall, these data therefore suggest that left-right medial prefrontal inhibitory connectivity might support in-depth visuospatial analyses—whose complexity reflects in the number of fixations[70]—aimed to evaluate, and make sense of, artistic ambiguous stimuli.

While further evidence is needed to unveil the neural bases of the multiple drivers of aesthetic appreciation, the present study provides novel cues into the behavioural and neural correlates of processing ambiguity in artistic photographic stimuli. In particular, our results suggest that the right superior parietal cortex, as well as left-right medial prefrontal inhibitory connectivity, might play a role in this aspect of visual cognition, possibly by mediating the (re)orientation of attention to global vs. local aspects[88] as well as in-depth visuospatial analysis of complex visual images[110]. The present findings therefore pave the way for future studies addressing the role of visual ambiguity in aesthetic appreciation, as well as the factors that might ease vs. hamper its processing and resolution, and their neural correlates.

Data availability

The datasets generated during the current study are available from the corresponding author on reasonable request.

Received: 14 September 2024; Accepted: 8 April 2025
Published online: 15 April 2025

References

1. Zeki, S. Art and the brain. *J. Conscious. Stud.* **6**(6–7), 76–96 (1999).
2. Boccia, M. et al. Where does brain neural activation in aesthetic responses to visual Art occur? Meta-analytic evidence from neuroimaging studies. *Neurosci. Biobehav. Rev.* **60**, 65–71 (2016).
3. Di Dio, C., Canessa, N., Cappa, S. F. & Rizzolatti, G. Specificity of esthetic experience for artworks: an fMRI study. *Front. Hum. Neurosci.* **5**, 139 (2011).
4. Chatterjee, A. & Vartanian, O. Neuroaesthetics. *Trends Cogn. Sci.*, **18**(7), 370–375. (2014).
5. Cattaneo, Z. Neural correlates of visual aesthetic appreciation: insights from non-invasive brain stimulation. *Exp. Brain Res.* **238**(1), 1–16 (2020).
6. Sacheli, L. M. et al. The unexplored link between aesthetic perception and creativity: a theory-driven meta-analysis of fMRI studies in the visual domain. *Neurosci. Biobehav. Rev.* **140**, 104768 (2022).
7. Kawabata, H. & Zeki, S. Neural correlates of beauty. *J. Neurophysiol.* **91**(4), 1699–1705 (2004).
8. Freedberg, D. & Gallese, V. Motion, emotion and empathy in esthetic experience. *Trends Cogn. Sci.* **11**(5), 197–203 (2007).
9. Zhang, W., Lai, S., He, X., Zhao, X. & Lai, S. Neural correlates for aesthetic appraisal of pictograph and its referent: an fMRI study. *Behav. Brain. Res.* **305**, 229–238 (2016).
10. Vartanian, O. & Goel, V. Neuroanatomical correlates of aesthetic preference for paintings. *Neuroreport* **15**(5), 893–897 (2004).
11. Kirk, U., Skov, M., Hulme, O., Christensen, M. S. & Zeki, S. Modulation of aesthetic value by semantic context: an fMRI study. *Neuroimage* **44**(3), 1125–1132 (2009).
12. Yang, T. et al. Aesthetic experiences across cultures: neural correlates when viewing traditional Eastern or Western landscape paintings. *Front. Psychol.* **10**, 798 (2019).
13. Kirk, U., Skov, M., Christensen, M. S. & Nygaard, N. Brain correlates of aesthetic expertise: a parametric fMRI study. *Brain Cogn.* **69**(2), 306–315 (2009).
14. Mullennix, J. W. & Robinet, J. Art expertise and the processing of titled abstract Art. *Perception* **47**(4), 359–378 (2018).
15. Huang, M., Bridge, H., Kemp, M. J. & Parker, A. J. Human cortical activity evoked by the assignment of authenticity when viewing works of Art. *Front. Hum. Neurosci.* **5**, 134 (2011).
16. Corradi, G., Chuquichambi, E. G., Barrada, J. R., Clemente, A. & Nadal, M. A new conception of visual aesthetic sensitivity. *Br. J. Psychol.* **111**(4), 630–658 (2020).
17. Nadal, M. & Vartanian, O. *The Oxford Handbook of Empirical Aesthetics* (Oxford University Press, 2022).
18. Palmer, S. E., Schloss, K. B. & Sammartino, J. Visual aesthetics and human preference. *Ann. Rev. Psychol.* **64**(1), 77–107 (2013).
19. Jacobsen, T., Schubotz, R. I., Höfel, L. & Cramon, D. Y. V. Brain correlates of aesthetic judgment of beauty. *Neuroimage* **29**(1), 276–285 (2006).
20. Balachander, N. *Sculptural Aesthetics and Neural Representation of Surface Curvature* (The Johns Hopkins University, 2012).
21. Palumbo, L. & Bertamini, M. The curvature effect: a comparison between preference tasks. *Empir. Stud. Arts*. **34**(1), 35–52 (2016).
22. Goldberg, E., Funk, B. A. & Podell, K. How the brain deals with novelty and ambiguity: implications for neuroaesthetics. *Rend. Lincei*. **23**, 227–238 (2012).
23. Yevin, I. Ambiguity in Art. *Complexus* **3**(1–3), 74–82 (2006).
24. Reber, R., Schwarz, N. & Winkielman, P. Processing fluency and aesthetic pleasure: is beauty in the perceiver's processing experience? *Personality Social Psychol. Rev.* **8**(4), 364–382 (2004).
25. Jakesch, M. & Leder, H. Finding meaning in Art: preferred levels of ambiguity in Art appreciation. *Q. J. Experimental Psychol.* **62**(11), 2105–2112 (2009).
26. Jakesch, M., Leder, H. & Forster, M. Image ambiguity and fluency. *PLoS One*, **8**(9), e74084. (2013).
27. Muth, C., Hesslinger, V. M. & Carbon, C. C. The appeal of challenge in the perception of art: How ambiguity, solvability of ambiguity, and the opportunity for insight affect appreciation. *Psychol. Aesthet. Creativity Arts* **9**(3), 206 (2015).

28. Stevanov, J., Marković, S. & Kitaoka, A. Aesthetic Valence of visual illusions. *i-Perception* **3**(2), 112–140 (2012).
29. Boccia, M. et al. *Why Do You Like Arcimboldo's Portraits?? Effect of Perceptual Style on Aesthetic Appreciation of Ambiguous Artworks* 761516–1521 (Attention, Perception, & Psychophysics, 2014).
30. Boccia, M., Guariglia, P., Piccardi, L., De Martino, G. & Giannini, A. M. The detail is more pleasant than the whole: Global and local prime affect esthetic appreciation of artworks showing whole-part ambiguity. Attention, Perception, & Psychophysics, 82(7), 3266–3272. (2020).
31. Boccia, M. et al. Do you like Arcimboldo's? Esthetic appreciation modulates brain activity in solving perceptual ambiguity. *Behav. Brain. Res.* **278**, 147–154 (2015).
32. Boccia, M., Barbetti, S., Piccardi, L., Guariglia, C. & Giannini, A. M. Neuropsychology of aesthetic judgment of ambiguous and non-ambiguous artworks. *Behav. Sci.* **7**(1), 13 (2017).
33. Van de Cruys, S. & Wagemans, J. Putting reward in Art: a tentative prediction error account of visual Art. *i-Perception* **2**(9), 1035–1062 (2011).
34. Berndt, F. & Koepnick, L. (eds) *Ambiguity in Contemporary Art and Theory, Vol. 16* (Felix Meiner, 2018).
35. Gamboni, D. *Potential Images: Ambiguity and Indeterminacy in Modern Art* (Reaktion Books, 2002).
36. Zeki, S. The neurology of ambiguity. *Conscious. Cogn.* **13**(1), 173–196 (2004).
37. Brascamp, J. W. & Shevell, S. K. The certainty of ambiguity in visual neural representations. *Annual Rev. Vis. Sci.* **7**(1), 465–486 (2021).
38. Wang, Y., Wang, L., Xu, Q., Liu, D. & Jiang, Y. Domain-specific genetic influence on visual-ambiguity resolution. *Psychol. Sci.* **25**(8), 1600–1607 (2014).
39. Díaz-Santos, M. et al. Effect of visual cues on the resolution of perceptual ambiguity in Parkinson's disease and normal aging. *J. Int. Neuropsychol. Soc.* **21**(2), 146–155 (2015).
40. Gori, S., Molteni, M. & Facoetti, A. Visual illusions: an interesting tool to investigate developmental dyslexia and autism spectrum disorder. *Front. Hum. Neurosci.* **10**, 175 (2016).
41. Grzeczkowski, L. et al. Is the perception of illusions abnormal in schizophrenia? *Psychiatry Res.* **270**, 929–939 (2018).
42. Dowdle, L. T., Ghose, G., Ugurbil, K., Yacoub, E. & Vizioli, L. Clarifying the role of higher-level cortices in resolving perceptual ambiguity using ultra high field fMRI. *NeuroImage* **227**, 117654 (2021).
43. Lebedev, M. A., Douglass, D. K., Moody, S. L. & Wise, S. P. Prefrontal cortex neurons reflecting reports of a visual illusion. *J. Neurophysiol.* **85**(4), 1395–1411 (2001).
44. von Gal, A. et al. Neural networks underlying visual illusions: an activation likelihood Estimation meta-analysis. *NeuroImage* **2023**, 120335 (2023).
45. Flounders, M. W., González-García, C., Hardstone, R. & He, B. J. Neural dynamics of visual ambiguity resolution by perceptual prior. *Elife* **8**, e41861 (2019).
46. González-García, C., Flounders, M. W., Chang, R., Baria, A. T. & He, B. J. Content-specific activity in frontoparietal and default-mode networks during prior-guided visual perception. *Elife* **7**, e36068 (2018).
47. Jakesch, M., Goller, J. & Leder, H. Positive fEMG patterns with ambiguity in paintings. *Front. Psychol.* **8**, 785 (2017).
48. Leder, H., Belke, B., Oeberst, A. & Augustin, D. A model of aesthetic appreciation and aesthetic judgments. *Br. J. Psychol.* **95**(4), 489–508 (2004).
49. Lisińska-Kuśnierz, M. & Krupa, M. Eye tracking in research on perception of objects and spaces. *Tech. Trans.* **115**(12), 5–22 (2018).
50. Lewis, G. *Street Photography: the Art of Capturing the Candid Moment* (Rocky Nook, Inc, 2015).
51. Dale, A. M. Optimal experimental design for event-related fMRI. *Hum. Brain. Mapp.* **8**(2-3), 109–114 (1999).
52. Nyström, M. & Holmqvist, K. An adaptive algorithm for fixation, saccade, and glissade detection in Eyetracking data. *Behav. Res. Methods.* **42**(1), 188–204 (2010).
53. Martinez-Conde, S., Macknik, S. L. & Hubel, D. H. The role of fixational eye movements in visual perception. *Nat. Rev. Neurosci.* **5**(3), 229–240 (2004).
54. Worsley, K. J. & Friston, K. J. Analysis of fMRI time-series revisited—again. *Neuroimage* **2**(3), 173–181 (1995).
55. Wilke, M. An alternative approach towards assessing and accounting for individual motion in fMRI timeseries. *Neuroimage* **59**(3), 2062–2072 (2012).
56. Friston, K. J., Stephan, K. E., Lund, T. E., Morcom, A. & Kiebel, S. Mixed-effects and fMRI studies. *Neuroimage* **24**(1), 244–252 (2005).
57. Chumbley, J., Worsley, K., Flandin, G. & Friston, K. Topological FDR for neuroimaging. *Neuroimage* **49**(4), 3057–3064 (2010).
58. Spisák, T. et al. Probabilistic TFCE: a generalized combination of cluster size and voxel intensity to increase statistical power. *Neuroimage* **185**, 12–26 (2019).
59. Smith, S. M. & Nichols, T. E. Threshold-free cluster enhancement: addressing problems of smoothing, threshold dependence and localisation in cluster inference. *Neuroimage* **44**(1), 83–98 (2009).
60. Eickhoff, S. B. et al. A new SPM toolbox for combining probabilistic cytoarchitectonic maps and functional imaging data. *Neuroimage* **25**(4), 1325–1335 (2005).
61. Tzourio-Mazoyer, N. et al. Automated anatomical labeling of activations in SPM using a macroscopic anatomical parcellation of the MNI MRI single-subject brain. *Neuroimage* **15**(1), 273–289 (2002).
62. Rolls, E. T., Huang, C. C., Lin, C. P., Feng, J. & Joliot, M. Automated anatomical labelling atlas 3. *Neuroimage* **206**, 116189 (2020).
63. Friston, K. J. et al. Psychophysiological and modulatory interactions in neuroimaging. *Neuroimage* **6**(3), 218–229 (1997).
64. Behzadi, Y., Restom, K., Liau, J. & Liu, T. T. A component based noise correction method (CompCor) for BOLD and perfusion based fMRI. *Neuroimage* **37**(1), 90–101 (2007).
65. Arioli, M., Basso, G., Poggi, P. & Canessa, N. Fronto-temporal brain activity and connectivity track implicit attention to positive and negative social words in a novel socio-emotional Stroop task. *Neuroimage* **226**, 117580 (2021).
66. Witt, S. T., van Ettinger-Veenstra, H., Salo, T., Riedel, M. C. & Laird, A. R. What executive function network is that? An image-based meta-analysis of network labels. *Brain Topogr.* **34**(5), 598–607 (2021).
67. Di Dio, C. The neural basis of the hedonic quality of aesthetic experience. *Rend. Lincei.* **23**, 271–280 (2012).
68. Menon, V. 20 Years of the default mode network: a review and synthesis. *Neuron* **111**(16), 2469–2487 (2023).
69. Sprugnoli, G. et al. Neural correlates of Eureka moment. *Intelligence* **62**, 99–118 (2017).
70. Koval, M. J., Hutchison, R. M., Lomber, S. G. & Everling, S. Effects of unilateral deactivations of dorsolateral prefrontal cortex and anterior cingulate cortex on saccadic eye movements. *J. Neurophysiol.* **111**(4), 787–803 (2014).
71. Wang, X., Bylinskii, Z., Hertzmann, A. & Pepperell, R. Toward quantifying ambiguities in artistic images. *ACM Trans. Appl. Percept. (TAP).* **17**(4), 1–10 (2020).
72. Di Dio, C., Macaluso, E. & Rizzolatti, G. The golden beauty: brain response to classical and renaissance sculptures. *PloS One*, **2**(11), e1201 (2007).
73. Corbetta, M., Kincade, J. M., Ollinger, J. M., McAvoy, M. P. & Shulman, G. L. Voluntary orienting is dissociated from target detection in human posterior parietal cortex. *Nat. Neurosci.* **3**(3), 292–297 (2000).
74. Corbetta, M. & Shulman, G. L. Control of goal-directed and stimulus-driven attention in the brain. *Nat. Rev. Neurosci.* **3**(3), 201–215 (2002).
75. Corbetta, M., Patel, G. & Shulman, G. L. The reorienting system of the human brain: from environment to theory of Mind. *Neuron* **58**(3), 306–324 (2008).

76. Ghosh, P., Roy, D. & Banerjee, A. Organization of directed functional connectivity among nodes of ventral attention network reveals the common network mechanisms underlying saliency processing across distinct Spatial and spatio-temporal scales. *NeuroImage* **231**, 117869 (2021).
77. Vossel, S., Geng, J. J. & Fink, G. R. Dorsal and ventral attention systems: distinct neural circuits but collaborative roles. *Neuroscientist* **20**(2), 150–159 (2014).
78. Gallese, V., Freedberg, D. & Umiltà, M. A. Embodiment and the aesthetic experience of images. *Brain, Beauty, and Art* **2022**, 88–92 (2022).
79. Di Dio, C. & Gallese, V. Moving toward emotions in the aesthetic experience. *Brain, Beauty Art: Essays Bringing Neuroaesthetics Focus* **2021**, 22–26 (2021).
80. Kirsch, L. P., Dawson, K. & Cross, E. S. Dance experience sculpts aesthetic perception and related brain circuits. *Ann. N. Y. Acad. Sci.* **1337**(1), 130–139 (2015).
81. Piechowski-Jozwiak, B., Boller, F. & Bogousslavsky, J. Universal connection through Art: role of mirror neurons in Art production and reception. *Behav. Sci.* **7**(2), 29 (2017).
82. Ticini, L. F., Urgesi, C. & Calvo-Merino, B. *Embodied Aesthetics: Insight From Cognitive Neuroscience Of Performing Arts. Aesthetics and the Embodied Mind: Beyond Art Theory And The Cartesian Mind-Body Dichotomy* 103–115 (Springer, 2015).
83. McAvoy, M. et al. Resting States affect spontaneous BOLD oscillations in sensory and paralimbic cortex. *J. Neurophysiol.* **100**(2), 922–931 (2008).
84. Fink, G. R. et al. Neural mechanisms involved in the processing of global and local aspects of hierarchically organized visual stimuli. *Brain: J. Neurol.* **120**(10), 1779–1791 (1997).
85. Pollmann, S. & Morrillo, M. Left and right occipital cortices differ in their response to Spatial cueing. *NeuroImage* **18**(2), 273–283 (2003).
86. Shen, L., Hu, X., Yacoub, E. & Ugurbil, K. Neural correlates of visual form and visual Spatial processing. *Hum. Brain. Mapp.* **8**(1), 60–71 (1999).
87. Ritzl, A. et al. Functional anatomy and differential time courses of neural processing for explicit, inferred, and illusory contours: an event-related fMRI study. *Neuroimage* **19**(4), 1567–1577 (2003).
88. Wu, Y. et al. The neuroanatomical basis for posterior superior parietal lobule control lateralization of visuospatial attention. *Front. Neuroanatomy* **10**, 32 (2016).
89. Harquel, S. et al. Modulation of visually induced self-motion illusions by α transcranial electric stimulation over the superior parietal cortex. *J. Cogn. Neurosci.* **36**(1), 143–154 (2024).
90. Bencivenga, F. et al. Effector-selective modulation of the effective connectivity within frontoparietal circuits during visuomotor tasks. *Cereb. Cortex.* **33**(6), 2517–2538 (2023).
91. Di Dio, C. et al. The neural correlates of velocity processing during the observation of a biological effector in the parietal and premotor cortex. *Neuroimage* **64**, 425–436 (2013).
92. Gallese, V. The conscious dorsal stream: embodied simulation and its role in space and action conscious awareness. *Psyche* **13**(1), 1–20 (2007).
93. Rizzolatti, G., Fogassi, L. & Vittorio Gallese. Parietal cortex: from sight to action. *Curr. Opin. Neurobiol.* **7**(4), 562–567 (1997).
94. Fox, M. D. & Raichle, M. E. Spontaneous fluctuations in brain activity observed with functional magnetic resonance imaging. *Nat. Rev. Neurosci.* **8**(9), 700–711 (2007).
95. Yeshurun, Y., Nguyen, M. & Hasson, U. The default mode network: where the idiosyncratic self Meets the shared social world. *Nat. Rev. Neurosci.* **22**(3), 181–192 (2021).
96. Camara, E., Rodriguez-Fornells, A., Ye, Z. & Münte, T. F. Reward networks in the brain as captured by connectivity measures. *Front. NeuroSci.* **3**, 875 (2009).
97. O'doherty, J. P. Reward representations and reward-related learning in the human brain: insights from neuroimaging. *Curr. Opin. Neurobiol.* **14**(6), 769–776 (2004).
98. Lacey, S. et al. Art for reward's sake: Visual art recruits the ventral striatum. *Neuroimage* **55**(1), 420–433 (2011).
99. Koepp, M. J. et al. Evidence for striatal dopamine release during a video game. *Nature* **393**(6682), 266–268 (1998).
100. Salimpoor, V. N., Benovoy, M., Larcher, K., Dagher, A. & Zatorre, R. J. Anatomically distinct dopamine release during anticipation and experience of peak emotion to music. *Nat. Neurosci.* **14**(2), 257–262 (2011).
101. Zeki, S., Romaya, J. P., Benincasa, D. M. & Atiyah, M. F. The experience of mathematical beauty and its neural correlates. *Front. Hum. Neurosci.* **8**, 68 (2014).
102. Comfort, W. E. & Freitas, A. L. *The Neuroscience of Beauty. Social and Affective Neuroscience of Everyday Human Interaction: From Theory to Methodology* 53–61 (Springer, 2022).
103. Vernet, M., Quentin, R., Chanes, L., Mitsumasu, A. & Valero-Cabré, A. Frontal eye field, where Art thou? Anatomy, function, and non-invasive manipulation of frontal regions involved in eye movements and associated cognitive operations. *Front. Integr. Nuerosci.* **8**, 66 (2014).
104. Moore, T. & Fallah, M. Microstimulation of the frontal eye field and its effects on Covert Spatial attention. *J. Neurophysiol.* **91**(1), 152–162 (2004).
105. Callan, A. M., Osu, R., Yamagishi, Y., Callan, D. E. & Inoue, N. Neural correlates of resolving uncertainty in Driver's decision making. *Hum. Brain. Mapp.* **30**(9), 2804–2812 (2009).
106. Slotnick, S. D. & Moo, L. R. Prefrontal cortex hemispheric specialization for categorical and coordinate visual Spatial memory. *Neuropsychologia* **44**(9), 1560–1568 (2006).
107. Bartel, G., Marko, M., Rameses, I., Lamm, C. & Riečanský, I. Left prefrontal cortex supports the recognition of meaningful patterns in ambiguous stimuli. *Front. NeuroSci.* **14**, 152 (2020).
108. Boroojerdi, B. et al. Enhancing analogic reasoning with rTMS over the left prefrontal cortex. *Neurology* **56**(4), 526–528 (2001).
109. Cerruti, C. & Schlaug, G. Anodal transcranial direct current stimulation of the prefrontal cortex enhances complex verbal associative thought. *J. Cogn. Neurosci.* **21**(10), 1980–1987 (2009).
110. Xiao, C., McNamara, T. P., Qin, S. & Mou, W. Neural mechanisms of recognizing scene configurations from multiple viewpoints. *Brain Res.* **1363**, 107–116 (2010).
111. Zacks, J. M., Vettel, J. M. & Michelon, P. Imagined viewer and object rotations dissociated with event-related fMRI. *J. Cognit Neurosci.* **15**, 1002–1018 (2003).
112. Shipman, S. L. & Astur, R. S. Factors affecting the hippocampal BOLD response during Spatial memory. *Behav. Brain. Res.* **187**(2), 433–441 (2008).

Acknowledgements

We wish to thank Manuel Zullo for his help in data collection. This research was partially supported by the "Ricerca Corrente" funding scheme of the Italian Ministry of Health.

Author contributions

MA: Conceptualization, Investigation, Data Collection, Analysis, Writing – original draft; NC: Conceptualization, Investigation, Supervision; Data Collection, Analysis, Methodology, Writing – original draft; AG: Data

Collection, Analysis, Methodology, Writing – editing; MZ: Data Collection, Analysis, Methodology; AF: Methodology, Resources; AS: Conceptualization, Investigation, Methodology, Resources, Supervision, Writing – editing.

Competing interests
The authors declare no competing interests.

Additional information
Supplementary Information The online version contains supplementary material available at https://doi.org/10.1038/s41598-025-97945-w.

Correspondence and requests for materials should be addressed to N.C.

Reprints and permissions information is available at www.nature.com/reprints.

Publisher's note Springer Nature remains neutral with regard to jurisdictional claims in published maps and institutional affiliations.